develop ecologically safe pest management strategies may have a considerable impact on future agricultural practices.

REFERENCES AND NOTES

1. G. N. Agrios, *Plant Pathology* (Academic Press, San Diego, ed. 3, 1988), pp. 3–39.
2. R. N. Goodman, Z. Király, K. R. Wood, *The Biochemistry and Physiology of Plant Infectious Disease* (Univ. of Missouri Press, Columbia, 1986), pp. 29–38.
3. R. C. Staples and V. Mako, *Exp. Mycol.* **4**, 2 (1980).
4. A. A. Bell and M. H. Wheeler, *Annu. Rev. Phytopathol.* **24**, 411 (1986).
5. S. Isaac, *Fungal-Plant Interactions* (Chapman & Hall, London, 1992), pp. 186–207.
6. J. M. Daly, *Annu. Rev. Phytopathol.* **22**, 273 (1984).
7. G. T. Cole, *Microbiol. Rev.* **50**, 95 (1986).
8. K. R. Dahlberg and J. L. Van Etten, *Annu. Rev. Phytopathol.* **20**, 281 (1982).
9. D. F. Farr, G. F. Bills, G. P. Chamuris, A. Y. Rossman, *Fungi on Plants and Plant Products in the United States* (American Phytopathological Society Press, St. Paul, MN, 1989).
10. R. J. O'Connel and J. A. Bailey, in *Biology and Molecular Biology of Plant-Pathogen Interactions*, J. Bailey, Ed. (Springer-Verlag, Berlin, 1986), pp. 39–48.
11. K. Erb, M. E. Gallegly, J. G. Leach, *Phytopathology* **63**, 1334 (1973).
12. S. F. Jenkins, Jr., and N. N. Winstead, *ibid.* **54**, 452 (1964).
13. S. Freeman and R. J. Rodriguez, *Plant Dis.* **76**, 901 (1992). Path-1 was originally designated HU25 and was derived from the wild-type isolate L2.5.
14. A. J. Anderson, in *Physiology and Biochemistry of Plant-Microbe Interactions*, N. T. Keen, T. Kosuge, L. L. Walling, Eds. (American Society of Plant Physiologists, Rockville, MD, 1988), pp. 103–110.
15. S. Freeman and R. J. Rodriguez, unpublished data.
16. R. C. Staples and H. C. Hoch, *Exp. Mycol.* **11**, 163 (1987).
17. M. R. Fernandez and M. C. Heath, *Can. J. Bot.* **64**, 648 (1985).
18. E. W. B. Ward, in (*10*), pp. 107–131.
19. J. W. Deacon, *Philos. Trans. R. Soc. London B* **318**, 249 (1988).
20. H. J. Hudson, *Fungal Biology* (Arnold, London, 1986), p. 298.
21. R. J. Rodriguez and J. L. Owen, *Exp. Mycol.* **16**, 291 (1992).
22. S. Freeman and J. Katan, *Phytopathology* **78**, 1656 (1988).

23. We thank N. Keen, R. Shaw, D. Ferrin, J. Menge, and G. Kurath for comments on the manuscript and R. D. Martyn for *Fusarium* isolates. Supported by grants from the United States–Israel Binational Agricultural Research and Development Fund (SI-0103-89) (S.F.), the University of California (UC) Regents, the UC, Riverside, Academic Senate, and the U.S. Department of Agriculture (9200655) (R.J.R.).

29 October 1992; accepted 12 January 1993

Skn-1a and Skn-1i: Two Functionally Distinct Oct-2–Related Factors Expressed in Epidermis

Bogi Andersen, Marcus D. Schonemann, Sarah E. Flynn, Richard V. Pearse II, Harinder Singh, Michael G. Rosenfeld

Two forms of a member of the POU domain family of transcriptional regulators, highly related to Oct-2, are selectively expressed in terminally differentiating epidermis and hair follicles. One form, referred to as Skn-1i, contains an amino-terminal domain that inhibits DNA binding and can inhibit transactivation by Oct-1. A second form, Skn-1a, contains an alternative amino terminus and serves to activate cytokeratin 10 (K10) gene expression. The pattern of expression of the *Skn-1a/i* gene products and the effect of the alternative products on the expression of other genes suggest that these factors serve regulatory functions with respect to epidermal development.

Although skin is the largest organ in mature mammals, epidermal development begins only on embryonic days (e) 15 to 16 during rat development (*1*). Before this stage, the primordium of epidermis consists of a bilayer of cells, a superficial layer referred to as periderm that is later shed, and a basal layer (*1, 2*). On e16, the basal cells begin to proliferate, generating a stratified epithelium in which characteristic subsets of genes, such as keratins, are differentially regulated in each layer (*1, 3*). Most of the suprabasal epidermal cells are postmitotic and eventually undergo programmed cell death, generating a superficial layer of dead cells (cornified epithelium) that appears on e18. This pattern of development, in which cells migrate to the surface during their differentiation only to undergo apoptosis, is continuously repeated in the adult, where the process is regulated by retinoic acid (*4*). Several transcription factors of wide distribution are expressed at high amounts in skin, including AP2, retinoic acid receptor γ, and retinoid X receptor α (*5*). However, cell-specific transcription factors that may be involved in epidermal cell maturation remain unknown.

The cloning of *Pit-1*, *Oct-1*, *Oct-2*, and *unc-86* led to the discovery of a gene family characterized by a bipartite DNA binding motif referred to as the POU domain (*6–14*). Unc-86, Pit-1, and Oct-2 are believed to be important in the terminal differentiation of neuronal, pituitary, and B lymphocyte cell types, respectively (*6, 7, 10, 11*). Oct-1 is a ubiquitous activator of gene programs required for cell proliferation (*12*) and may also play cell-specific roles (*13*). Subsequently, additional POU domain genes have been described in mammals, *Drosophila*, and *Caenorhabditis elegans*, most of which are transiently or selectively expressed in the developing nervous system (*14*).

Using screening by low stringency and polymerase chain reaction (PCR) of cDNAs from a number of tissues, we identified a cDNA clone distinct from known POU domain proteins (*15*). This cDNA clone contains a coding sequence predicting a 38-kD protein that is highly related to Oct-2 (Fig. 1). Whereas this protein differs from Oct-2 by only 15 amino acids over the POU-specific domain and the POU homeodomain, it is distinctly diverged from Oct-1 and Oct-2 in the linker region but contains regions of similarity outside the POU domain. To investigate the expression of this gene during development, we collected mouse embryos from blastocyst stage through e16.5, and PCR assays were performed by means of specific oligonucleotide primers (*16*) (Fig. 2A). This analysis revealed a biphasic pattern of expression: a signal was detected on e7.5, signal was low or undetectable between e9.5 and e12.5, and signal appeared again on e14.5. In addition, intense signal was observed in endometrium-placenta. In situ hybridization analyses with ^{35}S-labeled complementary RNA (cRNA) probe corresponding to the 3′ untranslated region of the gene (*17*) revealed no hybridization in rat embryos corresponding to the early phase of expression. However, there was intense hybridization at e17 in epidermal structures throughout the embryo, with no specific detectable hybridization in any other region (Fig. 2B). Evaluation at higher resolution revealed a dense pattern of silver grains over the epidermis but not over the dermal structures, with the most intense hybridization consistently observed over the most superficial layer of the epidermis (Fig. 2C). In developing embryos, a single, superficial layer of cells, the periderm, revealed no hybridization, whereas the adjacent, underlying ectoderm revealed intense hybridization. A transcript of 2.3 kb was observed in RNA blots of skin from neonatal mice (*18*). Using the more sensitive ribonuclease protection assay, we confirmed expression in epidermis, but no signal was detected in RNAs from the following adult organs from mice and rats: skeletal muscle, tongue, esophagus, heart, thymus, spleen, liver,

B. Andersen, M. D. Schonemann, S. E. Flynn, R. V. Pearse II, M. G. Rosenfeld, Eukaryotic Regulatory Biology Program, Howard Hughes Medical Institute, University of California School of Medicine, San Diego, La Jolla, CA 92093.
H. Singh, Howard Hughes Medical Institute, University of Chicago, Chicago, IL 60637.

kidney, testis, adrenals, placenta, lungs, brain, and anterior pituitary (*18*). In situ hybridization analyses of adult skin showed hybridization over suprabasal cells of the epidermis and intense hybridization in cortex cells of a subset of hair follicles (Fig. 2D). This pattern is consistent with a stage-specific expression during cyclical hair growth (*19*).

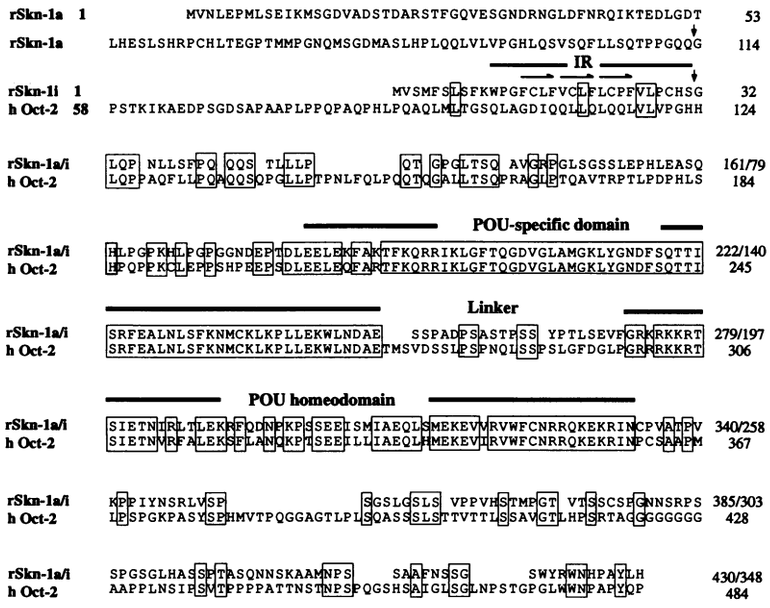

Fig. 1. Amino acid sequence of Skn-1a/i and comparison to Oct-2. The boxes show regions of complete sequence identity between rat Skn-1a/i and human Oct-2. Gaps were introduced for maximum alignment. The black bars indicate the POU-specific domain and the POU homeodomain with the linker region between the two bars. The black bar over the NH_2-terminus of Skn-1i represents a nonconserved inhibitory region (IR) for DNA binding. Horizontal arrows refer to an imperfect repeat in the inhibitory region. The vertical arrows show the point of divergence between Skn-1i and the product of alternative splicing, Skn-1a. Numbers represent the number of amino acids from the NH_2-terminus. Only amino acids 58 to 484 are shown for Oct-2. Abbreviations for the amino acid residues are as follows: A, Ala; C, Cys; D, Asp; E, Glu; F, Phe; G, Gly; H, His; I, Ile; K, Lys; L, Leu; M, Met; N, Asn; P, Pro; Q, Gln; R, Arg; S, Ser; T, Thr; V, Val; W, Trp; and Y, Tyr.

We evaluated the potential of the encoded protein to bind to an octamer site to which Oct-1 and Oct-2 bind with high affinity (*20*). The in vitro–translated protein was incapable of effectively binding to the immunoglobulin octamer-heptamer site in the gel mobility shift assay (*21*). However, a truncated form of the protein lacking the NH_2-terminal 60–amino acid residues bound to the octamer DNA sites with an affinity comparable to Oct-2 (Fig. 3A). These data suggested that the holoprotein, referred to as Skin-1i (Skn-1i), was inhibited from binding to octamer DNA sites by the NH_2-terminal sequence. Consistent with this idea, Skn-1i lacking the COOH-terminus was incapable of binding, whereas removal of the whole NH_2-terminus allowed DNA binding. Skn-1i holoprotein was unable to bind to any of a series of known POU domain DNA binding sites, including random oligonucleotides degenerate in 16 consecutive positions, as evaluated by gel mobility shift analyses. Skn-1i harboring a deletion of the first 32 amino acids had high affinity for all these sites (Fig. 3B). These data indicated that the POU domain of Skn-1i is competent to bind to octamer elements but is inhibited by information within the first 32 amino acids of Skn-1i.

To investigate whether this region constitutes a distinct inhibitory region, we transferred the NH_2-terminus of Skn-1i to another, unrelated transcription factor, thyrotroph embryonic factor (TEF), a member of the B-Zip gene family (*22*). The DNA binding ability of TEF, which binds

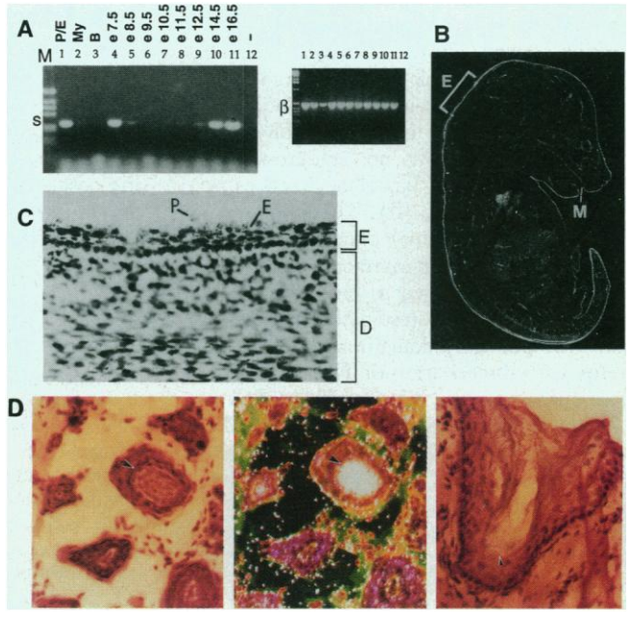

Fig. 2. Expression of *Skn-1a/i* mRNA. (**A**) RT PCR analyses of *Skn-1a/i* expression in the developing mouse embryo. Polyadenylated RNA was isolated from mouse uterus, placenta, and embryos from the indicated stages. We generated the cDNA using random oligonucleotides and RT. We used oligonucleotides specific for *Skn-1a/i* (S) to amplify a 236-bp POU domain fragment that was analyzed on a 2% agarose gel (left panel). As a control for the cDNA synthesis and the PCR reactions, we used oligonucleotides to amplify a 477-bp fragment specific for β-actin (right panel) (*16*). Markers (M) are a DNA ladder (in kilobases) (Bethesda Research Laboratories). P/E, placenta-endometrium; My, myometrium; B, blastocysts; and the minus sign indicates the negative control with no template added. (**B**) In situ hybridization analyses of *Skn-1a/i* expression. An e17 rat embryo was hybridized with an ^{35}S-labeled cRNA probe encompassing the 3′ untranslated region of *Skn-1a/i* (*17*). A dark-field photograph of a sagittal section is shown. Silver grains in the region above the heart and in the liver and brain are due to nonspecific adherence to red blood cells and edges, respectively. The absence of *Skn-1a/i* mRNA in brain and liver was confirmed by PCR RT analyses on tissues dissected from rat embryos. The epidermal-mucosal (M) junction that corresponds to the boundary of expression is indicated. Similar results were obtained with a probe corresponding to the most 5′ portion of the cDNA, whereas no signal was detected in epidermis when several unrelated cRNAs were used. E, epidermis. (**C**) A light-field photograph of a high magnification of skin from e17 rat embryo. Epidermis (E), dermis (D), and periderm cells (P) are indicated. (**D**) In situ hybridization analyses of *Skn-1a/i* expression in adult skin. The left (light field) and middle (dark field) panels show high magnification of hair follicles. Arrowheads point to a hair follicle showing intense hybridization. The panel to the right shows a high-magnification light-field photograph of epidermis at the entry point of a hair. Arrowhead points to silver grains that indicate specific hybridization.

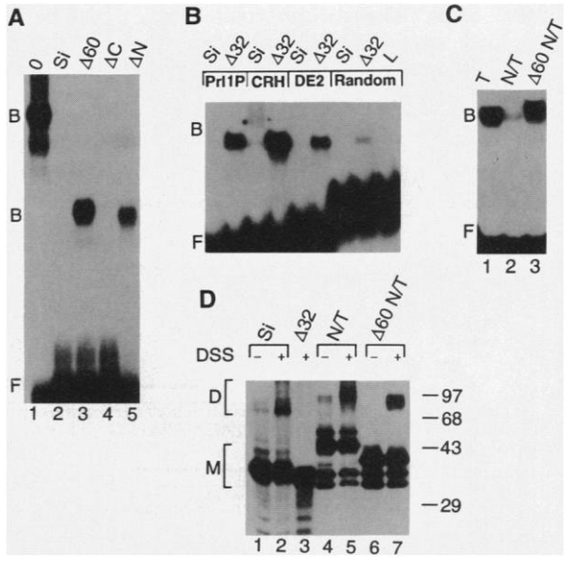

Fig. 3. The NH_2-terminus of Skn-1i contains a domain that inhibits DNA binding. (**A**) A gel mobility shift assay was performed with a ^{32}P-labeled oct-hep site and the indicated in vitro–translated proteins (*21*). O, Oct-2; Si, Skn-1i. Δ60, ΔC, and ΔN represent Skn-1i lacking the first 60 amino acids, the COOH-terminus, and the NH_2-terminus, respectively. We quantitated the ^{35}S-labeled proteins by TCA precipitation and analyzed by SDS-PAGE to ensure that equal amounts of protein were used in each binding reaction. The position of bound (B) and free (F) probes are indicated. No binding was detected even when the maximum concentrations of Skn-1i attainable in this assay were used. Equilibrium binding studies showed that the affinity of Oct-2 was two times higher than that of Δ60 Skn-1i (*18*). The ΔN Skn-1i contains amino acids 100 to 348 and ΔC Skn-1i contains amino acids 1 to 250. (**B**) A gel mobility shift analysis of the indicated ^{32}P-labeled sites (*21*) with equivalent amounts of Skn-1i holoprotein (Si) and Δ32 Skn-1i (Δ32). Because Δ32 Skn-1i binds specifically to only a small subset of the random sites, the bound complex is of low intensity, as expected for this technique. L is unprogrammed lysate. (**C**) Gel mobility shift analyses of TEF and Skn-1–TEF fusion proteins to a labeled Prl 1P site. T, wild-type TEF; N/T, amino acids 1 to 99 of Skn-1i fused to the NH_2-terminus site of TEF; Δ60 N/T, amino acids 61 to 99 of Skn-1i linked to TEF. (**D**) Solution cross-linking assay. The indicated ^{35}S-labeled proteins were incubated in the presence or absence of DSS cross-linker as indicated, and the products were analyzed by electrophoresis on a denaturing SDS–polyacrylamide gel (*23*). Minor bands most likely represent products initiated from internal methionines. Positions of monomers (M) and dimers (D) are indicated on the left side. The amount of dimer formed with N/T and Δ60 N/T was similar (13%). Migration of protein size standards is indicated at right in kilodaltons.

to AT-rich DNA sequences and readily forms homodimers and heterodimers, was entirely inhibited with the addition of the Skn-1i NH_2-terminal information. After subsequent removal of the initial 60 amino acids of Skn-1i, DNA binding was restored, suggesting that no other alterations in the structure of the cDNA encoding TEF had occurred during construction (Fig. 3C). Thus, the capacity of the initial 60 amino acids of Skn-1i to inhibit DNA binding could be transferred to a member of an entirely unrelated class of DNA binding proteins.

Next, the effect of the inhibitory region on dimerization in solution was assayed by the ability of a homobifunctional cross-linking agent, disuccinimydyl suberate (DSS), to cross-link in vitro–translated proteins (*23*). Although Skn-1i holoprotein exhibited cross-linking in solution in this dimerization assay, no such cross-linking was evident with Skn-1i lacking the first 32 amino acids (Fig. 3D). These data suggest that the inhibitory domain may provide a protein-protein interaction interface. Because TEF is known to bind DNA as a dimer (*22*), we also tested the hypothesis that the inhibitory domain acted by interfering with dimerization of TEF. Although TEF containing the NH_2-terminus of Skn-1i formed dimers less efficiently than TEF alone, no increase in dimerization was observed after removal of the initial 60 amino acids. Therefore, the effects of the inhibitory domain on TEF are selective for protein-DNA interaction rather than homodimer formation. Although inhibitory regions outside the DNA binding domain have not been previously described among POU proteins, this feature has been identified in other families of DNA binding proteins (*24–29*). However, the sequence of Skn-1i has no apparent similarity to these described inhibitory regions.

We constructed NH_2-terminal deletion mutants to further define the boundaries of the inhibitory domain. Serial truncations revealed that deletion of the first 11 amino acids did not allow binding, whereas maximum binding was observed after deletion of the first 32 amino acids. Therefore, a 21–amino acid region, extending from amino acids 11 to 32, was sufficient to confer inhibitory function. Deletions to amino acids 17 and 21 impaired but did not entirely eliminate inhibitory function, indicating that 11 amino acids are sufficient to

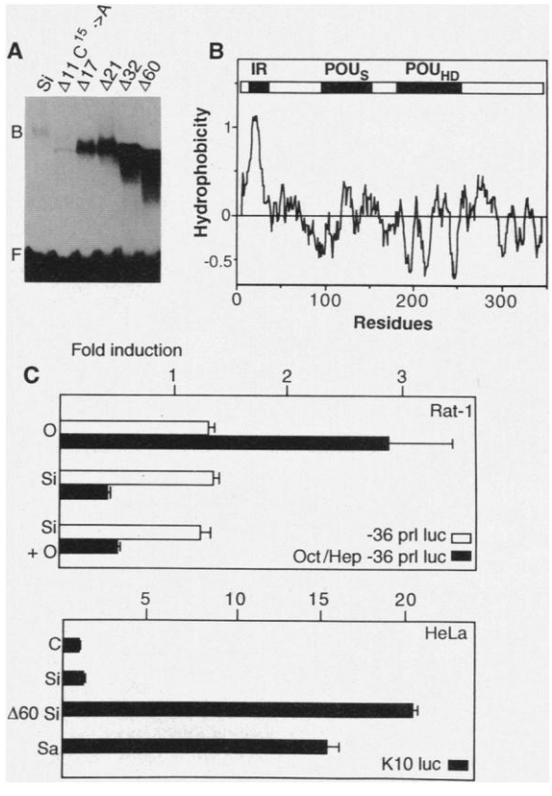

Fig. 4. Gel mobility shift analyses of NH_2-terminal truncation mutants and transient transfection assays. (**A**) Binding of the indicated in vitro–translated mutant proteins to a ^{32}P-labeled oct-hep element was assessed in the gel mobility–shift assay. Si, Skn-1i; Δ11, Δ17, Δ21, Δ32, and Δ60 are lacking the indicated number of amino acids from the NH_2-terminus of Skn-1i. In addition, Δ11 contained a mutation of Cys^{15} to an alanine. (**B**) A normalized Kyte-Doolittle hydropathy profile of Skn-1i. The POU-specific domain (POU_S) and the POU homeodomain (POU_{HD}) are indicated in addition to the IR. (**C**) The effect of Skn-1a/i in transient transfection assays (*31*). The indicated expression plasmids (0.5 μg) were transfected into Rat-1 (top panel) and HeLa (lower panel) cells with the indicated reporter plasmids (3.0 μg). Cells were harvested after 36 to 48 hours, and luciferase activity was measured. Results represent the mean ± SEM of quadruple determinations. O, cytomegalovirus (CMV) Oct-1; Si, CMV Skn-1i; C, CMV; Δ60 Si, CMV Skn-1i lacking amino acids 1 to 60 and Sa, CMV Skn-1a. K10 contains 1665 bp of 5′ flanking and untranslated sequence from the human cytokeratin 10 gene linked to luciferase (*33*); −36 prl luc contains the minimal prolactin promoter as described (*22*).

exert partial inhibitory function (Fig. 4A). Analysis by several algorithms, including a normalized Kyte-Doolittle hydropathy profile (*30*), revealed the inhibitory domain of Skn-1i to be highly hydrophobic (Fig. 4B). This region contains a four–amino acid motif repeated three times and four cysteines separated by three, three, and five amino acids with a subsequent histidine residue (Fig. 1), consistent with a potential zinc finger structure. However, a mutation of cysteine residue 15 did not allow DNA binding (Fig. 4A), and EDTA did not inhibit function of this domain (*18*). Therefore, zinc coordination is unlikely to be crucial for the function of this domain.

When the NH_2-terminal region of Skn-1i (from which the POU domain and COOH-terminus had been deleted) was mixed in ratios of 8:1 with intact TEF or a mutant Skn-1i lacking 32 amino acids from the NH_2-terminus (Δ32 Skn-1i), there was no inhibition of DNA binding, indicating that at this ratio the region did not act in trans to inhibit binding. Conversely, excess inhibitory domain did not permit binding of Skn-1i holoprotein, indicating that at these concentrations it could not saturate a second factor that could account for inhibition (*18*). These data are most consistent with the idea that the inhibitory domain of Skn-1i represents a region capable of altering the conformation of Skn-1i, possibly by forming intramolecular complexes and blocking the function of the helices involved in protein-DNA interactions. Because Skn-1i transcripts are most abundant in postmitotic cells of the superficial layer of the epidermis, we considered the possibility that it could inhibit the actions of Oct-1 that are thought to be important in cellular proliferation events (*12*). Transient cotransfection assays were conducted in a number of cell lines with plasmids containing Skn-1i and Oct-1 transcription units and a reporter gene under control of a minimal promoter and the immunoglobulin octamer-heptamer element. Oct-1 stimulated reporter gene expression in Rat-1 fibroblast cells and Skn-1i effectively inhibited this stimulation (*31*). The inhibition to the point below baseline is most likely due to inhibition of endogenous Oct-1. The precise molecular mechanisms for this inhibitory effect remain unknown. This inhibitory effect is specific because Skn-1i failed to inhibit the minimal promoter itself (Fig. 4C) or adenosine 3′,5′-monophosphate (cAMP) and estrogen response elements linked to the identical promoter (*18*). These data are consistent with the possibility that Skn-1i inhibits Oct-1's effects on gene expression in epidermis.

The high degree of conservation between the Skn-1i and Oct-2 POU domains suggested the existence of a form capable of binding DNA and positively regulating gene transcription. To search for an alternative form, we screened a neonatal rat skin cDNA library and identified a second transcript highly abundant in skin. This form, referred to as Skn-1a, is produced by alternative RNA splicing in which a 113–amino acid sequence replaces the initial 31 residues of Skn-1i (Fig. 1) (*32*). The potential activating role of Skn-1a was initially explored by cotransfection with genes under the control of a cytokeratin 10 (K10) promoter, which is a marker of terminally differentiating epidermal keratinocytes. In HeLa cells, Skn-1a was a potent activator of this promoter, whereas Skn-1i had a minimal effect (Fig. 4C). Because expression of a mutant Skn-1i lacking 60 amino acids from the NH_2-terminus (Δ60 Skn-1i) also activated the K10 promoter, it is likely that the critical function of the Skn-1a NH_2-terminus is to relieve the action of the Skn-1i inhibitory domain rather than to serve as a transactivation domain. Skn-1a/i thus represent tissue-restricted POU domain factors that may exert selective activating and inhibiting functions in developing epidermis.

REFERENCES AND NOTES

1. R. Kopan and E. Fuchs, *Genes Dev.* **3**, 1 (1989).
2. P. Davidson and M. H. Hardy, *J. Anat. Physiol.* **86**, 342 (1952).
3. E. Fuchs, *Trends Genet.* **4**, 277 (1988).
4. _____ and H. Green, *Cell* **25**, 617 (1981); G. J. Fisher *et al.*, *J. Invest. Dermatol.* **96**, 699 (1991).
5. P. J. Mitchell, P. M. Timmons, J. M. Hebert, P. S. J. Rigby, R. Tjian, *Genes Dev.* **5**, 105 (1991); A. Leask, C. Byrne, E. Fuchs, *Proc. Natl. Acad. Sci. U.S.A.* **88**, 7948 (1991); A. Zelent, A. Krust, M. Petkovich, P. Kastner, P. Chambon, *Nature* **339**, 714 (1989); A. Krust, P. H. Kastner, M. Petkovich, A. Zelent, P. Chambon, *Proc. Natl. Acad. Sci. U.S.A.* **86**, 5310 (1989); D. J. Mangelsdorf *et al.*, *Genes Dev.* **6**, 329 (1992).
6. R. A. Sturm, G. Das, W. Herr, *Genes Dev.* **2**, 1582 (1988); H.-S. Ko, P. Fast, W. McBride, L. M. Staudt, *Cell* **55**, 135 (1988); R. G. Clerc, L. M. Corcoran, J. H. LeBowitz, D. Baltimore, P. A. Sharp, *Genes Dev.* **2**, 1570 (1988); C. Scheidereit *et al.*, *Nature* **336**, 551 (1988); M. M. Müller, S. Ruppert, W. Schaffner, P. Matthias, *ibid.*, p. 544.
7. H. A. Ingraham *et al.*, *Cell* **55**, 519 (1988); M. Bodner *et al.*, *ibid.*, p. 505.
8. M. Finney, G. Ruvkun, H. R. Horvitz, *ibid.*, p. 757.
9. R. A. Sturm and W. Herr, *Nature* **336**, 601 (1988); H. A. Ingraham *et al.*, *Cell* **61**, 1021 (1990); C. P. Verrijzer, A. J. Kal, P. C. van der Vliet, *Genes Dev.* **4**, 1964 (1990); R. Aurora and W. Herr, *Mol. Cell. Biol.* **12**, 455 (1992); J. W. Voss, L. Wilson, M. G. Rosenfeld, *Genes Dev.* **5**, 1309 (1991); C. P. Verrijzer, J. A. W. M. van Oosterhout, P. C. van der Vliet, *Mol. Cell. Biol.* **12**, 542 (1992).
10. M. Finney and G. Ruvkun, *Cell* **63**, 895 (1990).
11. S. Li *et al.*, *Nature* **347**, 528 (1990).
12. M. Tanaka, U. Grossniklaus, W. Herr, N. Hernandez, *Genes Dev.* **2**, 1764 (1988); C. Fletcher, N. Heintz, R. G. Roeder, *Cell* **51**, 773 (1987); C. P. Verrijzer, A. J. Kal, P. C. van der Vliet, *EMBO J.* **9**, 1883 (1990).
13. Y. Luo, F. Hiroshi, T. Gerster, R. G. Roeder, *Cell* **71**, 231 (1992).
14. H. R. Schöler, *Trends Genet.* **7**, 323 (1991); M. G. Rosenfeld, *Genes Dev.* **5**, 897 (1991); G. Ruvkun and M. Finney, *Cell* **64**, 475 (1991).
15. RNA was isolated from several rat tissues, including embryonic head and anterior pituitary. Complementary DNA was synthesized, and we used oligonucleotides corresponding to conserved regions of the POU domain to amplify POU domains. Among the POU domains obtained with this approach were Oct-1 and Oct-2. These fragments were ^{32}P-labeled, and we used them in combination to screen under low stringency ~500,000 plaques from a rat pituitary cDNA library. Using this approach, we obtained two clones, Oct-1 and a 2194-bp-long cDNA. Both strands of the unknown cDNA clone were sequenced by means of dideoxy nucleotides [F. Sanger, S. Nicklen, A. R. Coulson, *Proc. Natl. Acad. Sci. U.S.A.* **74**, 5463 (1977)] and Sequenase (U.S. Biochemicals). This cDNA contained a single open reading frame of 1044 bp in addition to 277 bp and 873 bp of 5′ and 3′ untranslated sequence, respectively. The predicted amino acid sequence of the POU domain was similar to a partial POU domain PCR product from mouse testis [A. Goldsborough, A. Ashworth, K. Willison, *Nucleic Acids Res.* **18**, 1634 (1990)]. This cDNA most likely contains a full coding region because there are in-frame stops 5′ to the initial methionine. Furthermore, there is good agreement between the size of the cDNA and the size of the transcript (2.3 kb), as determined by Northern (RNA) analyses (*18*).
16. Blastocysts and mouse embryos were isolated by standard techniques [B. Hogan, F. Costantini, E. Lacy, *Manipulating the Mouse Embryo: A Laboratory Manual* (Cold Spring Harbor Laboratory, Cold Spring Harbor, NY, 1986)]. Polyadenylated RNA was isolated by means of the Micro Fast Track kit (Invitrogen), and cDNAs were synthesized with random hexamers and reverse transcriptase (RT) (Superscript RT, Bethesda Research Laboratories), both used according to the instructions from the vendors. This cDNA was used as a template for the PCR with primers specific for the mouse *Skn-1i* POU domain (sense: 5′-TAAAGCTTGTTGAATGATGCAGAGTCCTCCCCG-3′; antisense: 5′-ATGGATCCCACCACCTCCTTCTCCATCGAT-3′) or β-actin (sense: 5′-GATCGAATTCGACGAGGCGCAGAGCAAGAGAGG-3′; antisense: 5′-GATCGGATCCCTCTTTGATGTCACGCACGATTTC-3′). Primers flanked introns to avoid priming from genomic DNA.
17. Rat embryos were immersion-fixed in 10% buffered formalin, and 10- to 30-μm-thick frozen sections were cut in a cryostat. In situ hybridizations were done as described with ^{35}S-labeled cRNA probes [D. M. Simmons, J. L. Arriza, L. W. Swanson, *J. Histotechnol.* **12**, 169 (1989)]. One antisense probe corresponded to the 5′ untranslated region and the beginning of the coding region (nucleotides 1 to 379), and the other corresponded to the 3′ untranslated region (nucleotides 1475 to 2194). After hybridization, slides were dipped in NTB-2 liquid autoradiography emulsion (Kodak, New Haven, CT) and exposed for 5 to 7 days.
18. B. Andersen and M. G. Rosenfeld, unpublished data.
19. M. H. Hardy, *Trends Genet.* **8**, 55 (1992).
20. R. Sturm, T. Baumruker, B. R. Franza, Jr., W. Herr, *Genes Dev.* **1**, 1147 (1987); T. Baumruker, R. Sturm, W. Herr, *ibid.* **2**, 1400 (1988); J. H. LeBowitz, R. G. Clerc, M. Brenowitz, P. A. Sharp, *ibid.* **3**, 1625 (1989); L. Poellinger and R. G. Roeder, *Mol. Cell. Biol.* **9**, 747 (1989).
21. We generated the full-length *Skn-1i* cDNA and deletion mutants either by taking advantage of convenient restriction sites or by using the PCR in conjunction with specific primers. Coding sequences were cloned into a T7 expression vector containing a methionine for initiation in vitro (*22*). Proteins were synthesized in vitro in the presence of [^{35}S]methionine with rabbit reticulocyte lysate treated with nuclease. Proteins were quantitated by trichloroacetic acid (TCA) precipitation and SDS–polyacrylamide gel electrophoresis (PAGE). Generally, 0.5 to 2 μl of programmed lysate were used for gel mobility shift assays. Gel mobility shift assays were done as described [V. C. Yu *et al.*, *Cell* **67**, 1251 (1991)] except that binding reac-

tions without probe were first incubated for 20 min on ice. Sequences of the octamer-heptamer (octhep), Prl 1P, and CRH sites were as described [J. M. Mathis, D. Simmons, X. He, L. W. Swanson, M. G. Rosenfeld, *EMBO J.* **11**, 2551 (1992)]. The DE2 site is 5′-GAGTGGAGATCCAACAGCATCCTTAATTAAGTTCCT-3′.
22. D. W. Drolet *et al.*, *Genes Dev.* **5**, 1739 (1991).
23. Approximately 100,000 cpm of ^{35}S-labeled protein were added at room temperature to 20 μl of binding buffer [10 mM Hepes (pH 7.8), 50 mM KCl, and 5% glycerol]. After 15 min at room temperature, 0.5 μl of DSS in dimethyl sulfoxide (DMSO; 5 mg/ml) or DMSO alone was added to the reactions. After 5 min, we stopped the reaction by adding SDS sample buffer (*22*). The sample was boiled before analyses by SDS-PAGE. To quantitate cross-linking efficiency, we excised monomers and dimers from the gel and measured them by scintillation counting.
24. X.-H. Sun and D. Baltimore, *Cell* **64**, 459 (1991).
25. C. Wasylyk, J.-P. Kerckaert, B. Wasylyk, *Genes Dev.* **6**, 965 (1992).
26. S. M. Ruben *et al.*, *ibid.*, p. 745.
27. H.-C. Liou *et al.*, *EMBO J.* **11**, 3003 (1992).
28. P. A. Baeuerle and D. Baltimore, *Science* **242**, 540 (1988); S. Ghosh and D. Baltimore, *Nature* **344**, 678 (1990); L. D. Kerr *et al.*, *Genes Dev.* **5**, 1464 (1991); M. B. Urban and P. A. Baeuerle, *ibid.* **4**, 1975 (1990); U. Zabel and P. A. Baeuerle, *Cell* **61**, 255 (1990).
29. D. Picard, S. J. Salser, K. R. Yamamoto, *Cell* **54**, 1073 (1988); W. B. Pratt *et al.*, *J. Biol. Chem.* **263**, 267 (1988).
30. J. Kyte and R. F. Doolittle, *J. Mol. Biol.* **157**, 105 (1982).
31. Rat-1 cells were plated at low density the day before transfection. Transfections were performed by the calcium phosphate method as described (*22*). Cells were harvested after 48 hours, and luciferase activity measured. HeLa cells were transfected with the lipofectant DOTAP (Boehringer Mannheim) according to the manufacturer's instructions. Cells were harvested after 36 to 48 hours.
32. We used RNA from rat neonatal skin with random hexamers and avian myeloblastosis virus RT to generate cDNA that was cloned into λZAP II (Stratagene). This library was screened with a ^{32}P-labeled probe corresponding to the entire NH_2-terminus and the POU domain of Skn-1i. Three independent clones were isolated that together corresponded to the entire common region between Skn-1i and Skn-1a. One of the clones, Skn-1a, contained a 5′-sequence that predicted a different NH_2-terminus as a result of alternative splicing. The expression of both forms in skin was demonstrated with the PCR with primers specific for each form and with RNA hybridization studies (*18*).
33. M. Rieger and W. Franke, *J. Mol. Biol.* **204**, 841 (1988).
34. We thank P. Sawchenko for advice on in situ technology and photography; K. Jenne and S. O'Connell for blastocyst isolates and help with in situ hybridization; C. Nelson for tissue culture; D. Drolet for TEF plasmids and helpful discussions; and S. Lipkin, A. Näär, A. Hariri, and S. Hunt for suggestions. B.A. is supported by a Bugher American Heart Association Fellowship; M.G.R. is an investigator with The Howard Hughes Medical Institute. Supported in part by NIH grant number DK39949.

23 September 1992; accepted 18 December 1992

Rhythmic Exocytosis Stimulated by GnRH-Induced Calcium Oscillations in Rat Gonadotropes

Amy Tse, Frederick W. Tse, Wolfhard Almers, Bertil Hille*

In pituitary gonadotropes, gonadotropin-releasing hormone (GnRH) induces the rhythmic release of Ca^{2+} from an inositol 1,4,5-trisphosphate (IP_3)–sensitive store. Simultaneous measurement of the concentration of cytosolic free Ca^{2+} ($[Ca^{2+}]_i$) and exocytosis in single identified gonadotropes showed that each elevation of $[Ca^{2+}]_i$ induced a burst of exocytosis. These phenomena were largely suppressed by buffering of $[Ca^{2+}]_i$ but persisted in the absence of extracellular Ca^{2+}. Activation of voltage-gated Ca^{2+} channels by brief depolarizations seldom supplied enough Ca^{2+} for exocytosis, but $[Ca^{2+}]_i$ elevations induced by photolysis of caged IP_3 did trigger exocytosis, confirming that GnRH-stimulated gonadotropic hormone secretion is closely coupled to intracellular Ca^{2+} release. Agonist-induced oscillations of $[Ca^{2+}]_i$ in secretory cells may be a mechanism to optimize the secretory output while avoiding the toxic effects of sustained elevation of $[Ca^{2+}]_i$.

Although many cells display oscillations in $[Ca^{2+}]_i$ in response to agonists, physiological roles for these oscillations are unclear (*1*). Pituitary gonadotropes exhibit oscillations in $[Ca^{2+}]_i$ in response to their natural stimulating hormone, GnRH (*2*). Each cycle of increase in $[Ca^{2+}]_i$ hyperpolarizes the cell by opening apamin-sensitive Ca^{2+}-activated K^+ channels (*3–5*). This allows voltage-gated Na^+ and Ca^{2+} channels to recover from inactivation and then to fire action potentials when $[Ca^{2+}]_i$ declines again and the cell depolarizes (*5*). Thus, GnRH stimulates both the entry of extracellular Ca^{2+} through voltage-gated Ca^{2+} channels and the release of intracellular Ca^{2+} in gonadotropes. Understanding the relative contribution of these mechanisms to GnRH-induced secretion of gonadotropic hormones (*6*), and particularly whether each cycle of increase in $[Ca^{2+}]_i$ can trigger secretion, has been difficult because of the low temporal resolution of traditional assays for hormone secretion. We used high temporal resolution capacitance measurements (*7*), which monitor changes in cell membrane capacitance (ΔC_m) resulting from exocytosis of secretory vesicles, to measure simultaneously exocytosis and $[Ca^{2+}]_i$ in identified gonadotropes of adult male rats (*8*).

GnRH-induced $[Ca^{2+}]_i$ oscillations are readily seen with fluorescent indicators, even in gonadotropes voltage-clamped to potentials (−90 mV) at which voltage-gated Ca^{2+} channels are closed. A 10-s application of GnRH caused $[Ca^{2+}]_i$ to oscillate (Fig. 1A). In 40 cells, the resting $[Ca^{2+}]_i$ was 109 ± 16 nM, and the maximal $[Ca^{2+}]_i$ induced by a brief application of GnRH (40 or 50 nM) was 3.3 ± 0.2 μM. The rising phase of each cycle of $[Ca^{2+}]_i$ elevation was accompanied by an increase in C_m (Fig. 1B) and by an increase in the rate of exocytosis ($\Delta C_m/\Delta t$) (Fig. 1C). In later cycles of the $[Ca^{2+}]_i$ oscillation (for

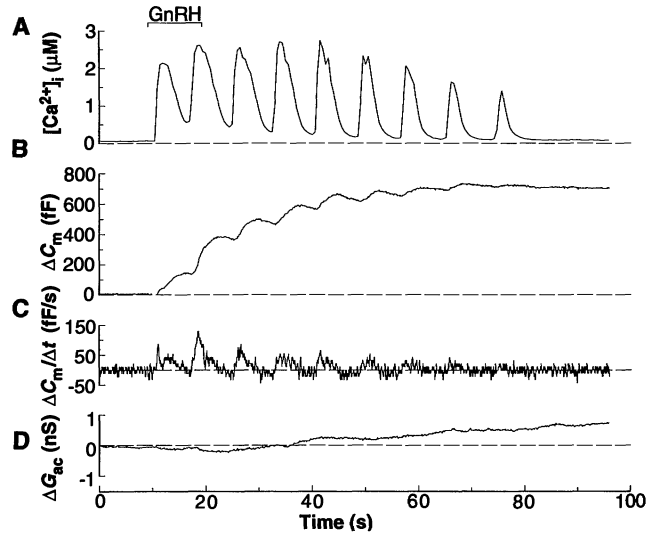

Fig. 1. Time course of GnRH-induced oscillations in $[Ca^{2+}]_i$ and accompanying bursts of exocytosis. (**A**) $[Ca^{2+}]_i$. (**B**) ΔC_m. (**C**) $\Delta C_m/\Delta t$. (**D**) ΔG_{ac}. GnRH (40 nM) was applied during the 10-s period marked with a bar. The initial membrane capacitance was 6.8 pF. To reduce contamination of capacitance signal by conductance changes, we voltage-clamped the cell at a holding potential of −90 mV to shut off most voltage-gated ionic channels, and the GnRH-induced rhythmic increase in Ca^{2+}-activated K^+ conductance was blocked by extracellular apamin and TEA (*3*). Ionic conductance changes were indeed minimal under these conditions (ΔG_{ac} trace).

A. Tse, F. W. Tse, B. Hille, Department of Physiology and Biophysics, University of Washington School of Medicine, SJ-40, Seattle, WA 98195.
W. Almers, Max-Planck-Institut für Medizinische Forschung, 6900 Heidelberg, Germany.
*To whom correspondence should be addressed.